



REPAIR OF HIGH-STRENGTH REINFORCED CONCRETE BEAM-COLUMN JOINTS

K. TABATA and T. NAKACHI

Technical Research Institute, HAZAMA Corporation, 515-1, Nishimukai, Karima,
Tsukuba, Ibaraki, 305, Japan

ABSTRACT

In order to investigate the earthquake resisting ability of high-strength reinforced concrete members after repair, loading tests of interior beam-column joints were carried out. The variables were the concrete compressive strength and number of main bars of the beam. After repair of damaged specimens using low viscous epoxy resin and non-shrinking high-strength mortar, the second series of loading tests were carried out. The performance of repaired specimens whose joint shear deformation were not large during the original loading, was as good as that of the original specimens.

KEYWORDS

Repair; high-strength; beam-column joint; epoxy resin; non-shrinking mortar; reinforced concrete.

INTRODUCTION

Many reinforced concrete structures damaged by earthquake are able to be made usable by repair. In regard to normal strength reinforced concrete members, many studies have been performed, and the effectiveness of such repair has been reported (Tasai, 1992). Though research and development on high strength concrete members has been carried out, the structural characteristics of these members after repair has not been well researched. In this study the loading tests of high-strength reinforced concrete beam-column joints were carried out, and the performance of these members before and after repair were compared and the effectiveness of repair was evaluated.

TEST PROGRAM

Specimens

The properties of specimens are summarized in Table 1. The arrangement of reinforcement of specimens and member sections are shown in Fig.1. The specimens before and after repair are numbered 1 to 6 and

Table 1. Properties of Specimens

Specimen	Design Concrete Strength F_c (MPa)	Beam			Column			Joint	
		Main Bar	Stirrup	$P_w(\%)$	Main Bar	Hoop	$P_w(\%)$	Hoop	$P_w(\%)$
No. 1	41.2	4-D19	4-U6.4065	0.62	16-D19	4-U6.4050	0.60	4-U5.1033	0.59
No. 2	41.2	6-D19	4-U6.4065	0.62	16-D19	4-U6.4050	0.60	4-U5.1033	0.59
No. 3	35.3	4-D19	4-6.4 ϕ 065	0.62	16-D19	4-6.4 ϕ 050	0.60	4-U5.1033	0.59
No. 4	35.3	6-D19	4-6.4 ϕ 065	0.62	16-D19	4-6.4 ϕ 050	0.60	4-U5.1033	0.59
No. 5	58.8	6-D19	4-6.4 ϕ 065	0.62	16-D19	4-6.4 ϕ 050	0.60	4-U5.1033	0.59
No. 6	58.8	8-D19	4-6.4 ϕ 065	0.62	16-D19	4-6.4 ϕ 040	0.75	4-U5.1033	0.59

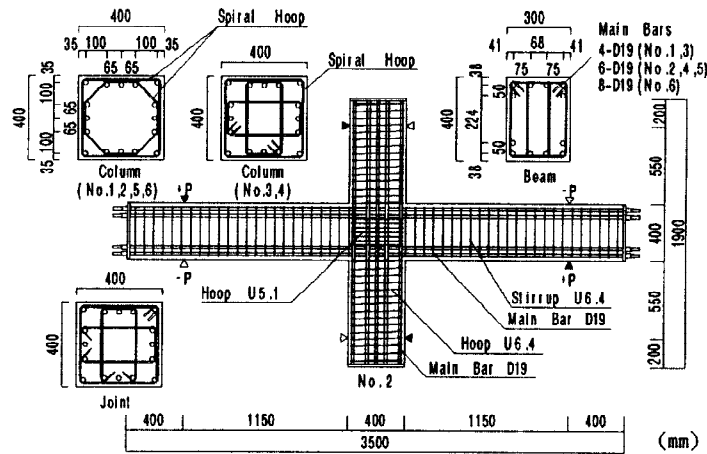


Table 1. Arrangement of Reinforcement

Table 2. Material Properties

Concrete				Steel				
Specimen	Compressive Strength σ_B (MPa)	Young's Modulus* (MPa)	Split Strength (MPa)	Bar Size	Yield Strength (MPa)	Maximum Strength (MPa)	Young's Modulus (MPa)	Elongation (%)
No. 1	44.5	3.46×10^4	2.83	D19	493	653	1.94×10^5	19.4
No. 2	47.5	3.52×10^4	3.13	U6.4**	1348	1494	2.04×10^5	9.0
No. 3	30.8	2.78×10^4	2.28	U5.1**	1364	1471	2.06×10^5	9.8
No. 4	32.3	2.83×10^4	2.34	6.4 ϕ **	1384	1432	2.00×10^5	9.3
No. 5	60.3	3.81×10^4	3.56					
No. 6	64.5	3.87×10^4	3.72					

* Secant modulus at one-third of σ_B

** 0.002 off set

1R to 6R respectively. A half-scale interior beam-column joint made from high strength material was used as the specimen for this experiment. The specimens represent the portion of lower stories of high-rise structures of approximately fifteen to fifty stories. The variables were the specified design concrete strength F_c (35.3, 41.2, 58.5MPa) and number of beam main bars. High strength bars with a yield strength of 493MPa and 1300MPa were used for longitudinal and transverse reinforcement respectively. The material properties are listed in Table 2. The specimens were designed so that the beam flexural yielding would occur prior to shear failure in the joints.

Loading Method

The loading apparatus and the loading history are shown in Fig.2. Both the original and the repaired specimens were loaded by the same method. The ends of two beams were loaded by two hydraulic jacks in the opposite direction so that the vertical displacement might be kept identical. During the loading the points of contraflexure of the columns were pinned. A constant axial load was applied to the top of the column by hydraulic jack. With the exception of specimen 6, during the original loading, the axial stress σ_o was 20% of the concrete compressive cylinder strength σ_B (specimen 6: $\sigma_o = 0.19 \sigma_B$, $\sigma_o = N/A$, N: the axial load, A: the column cross sectional area). The same axial loads were applied to the original specimens and repaired specimens respectively.

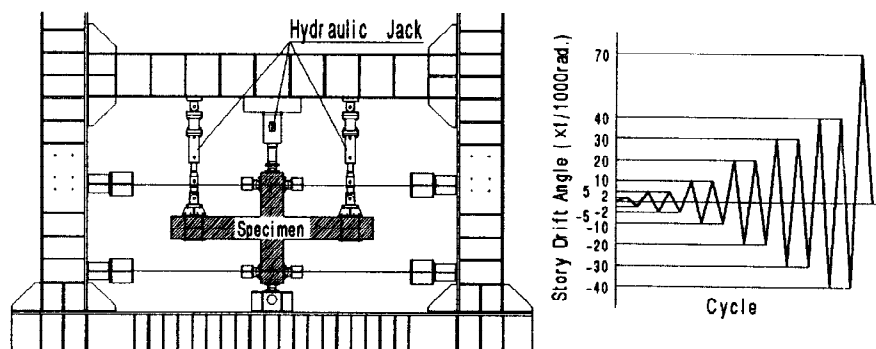


Fig.2. Loading Apparatus and Loading History

Table 3. Properties and Quantities of Epoxy Resin and High-Strength Non-Shrinking Mortar

	Compressive Strength (MPa)	Young's Modulus* (MPa)	Tensile Strength (MPa)	Quantity of Injection Volume of Specimen					
				No. 1	No. 2	No. 3	No. 4	No. 5	No. 6
Epoxy Resin	84.8	0.23×10^4	46.8	0.12%	0.18%	0.20%	0.26%	0.24%	0.29%
Mortar	69.6	2.50×10^4	3.94	5.41%	7.07%	5.52%	6.72%	5.75%	5.95%

*Secant modulus at one-third of the compressive strength

Table 4. Test Results

Specimen	Cracking Load (kN)			Yield of Beam Main Bar		Maximum Load Pmax (kN)	Final Failure Mode*
	Beam Flexural	Column Flexural	Joint Shear	Load (kN)	drift ($\times 1/1000\text{rad.}$)		
No. 1	39	127	142	168	8.1	179	BB ₀ *
No. 2	40	127	139	233	9.5	252	BJ**
No. 3	29	98	127	168	9.5	169	BB ₀ *
No. 4	27	97	107	220	14.1	229	BJ**
No. 5	51	158	165	231	7.7	259	BB ₀ *
No. 6	41	178	167	282	9.1	330	BJ**

*BB₀: Bond splitting failure of a joint after beam flexural yielding

** BJ: Shear compression failure of a joint after beam flexural yielding

Repair Method

The residual deformation of specimens due to original loading was corrected so that the drift angle would become zero. The crushed concrete of specimens was removed. After the cracks of the beams, columns and joints were covered with sealing compound, low viscous epoxy resin was injected into the cracks. The sealing compound and the concrete around hoops of joints and stirrups of beams were removed. To restore the original shape, forms were set and the cavities filled with non-shrinking high-strength mortar. The properties and quantities of epoxy resin and mortar used for repair, are listed in Table 3. The material tests were carried out in accordance with Japanese Industrial Standards.

TEST RESULTS AT THE ORIGINAL LOADING

Failure progress

The test results at the original loading are listed in Table 4. In the table, the loads represent values at forward loading, and the beam main bars are outer-layer reinforcement. The crack patterns of original specimens after test are shown in Fig.3. Fig.4 shows the load-deflection curve. Dashed lines and solid lines in figure are the results before and after repair respectively. The load is the average of two forces applied to the beam ends by the jacks. The vertical deflection is the average of beam end displacement divided by half the distance between the two loading points. The displacement was measured by the transducers fixed on a frame pinned at the points of contraflexure of the column.

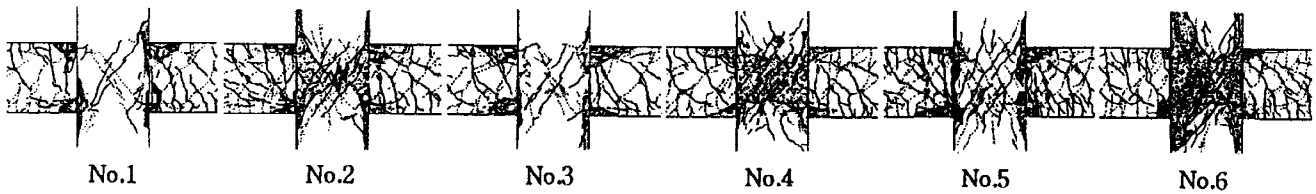


Fig.3. Crack Patterns of Original Specimens

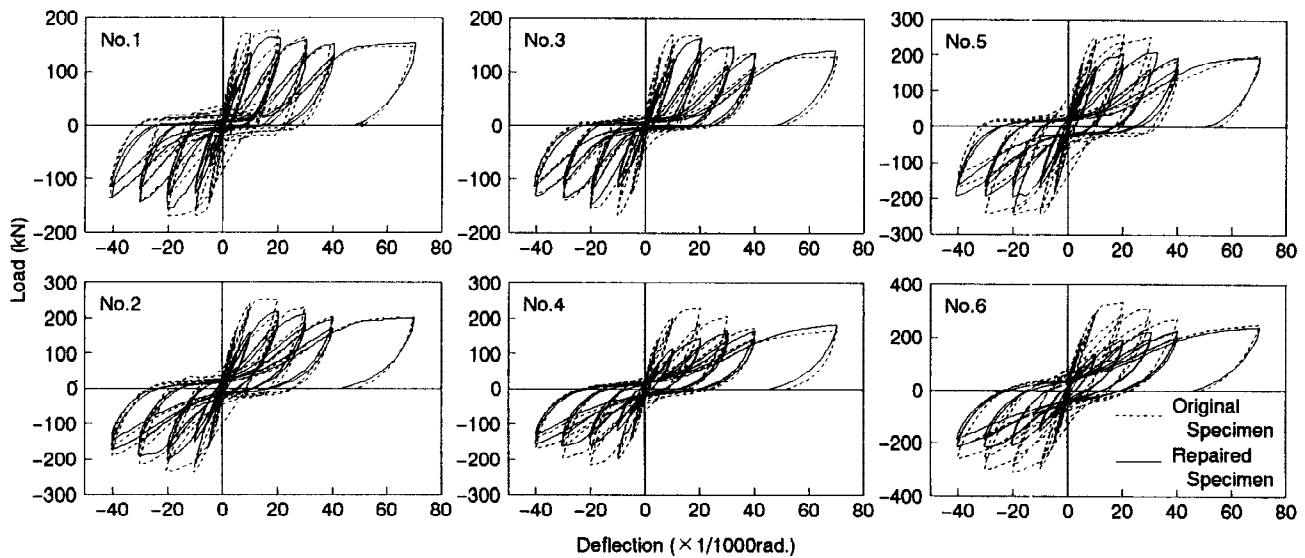


Fig.4. Load-Deflection Curve

In all specimens, the beam flexural cracks occurred at cycle R (a drift angle) $=2/1000$ (rad.), the column flexural cracks and joint shear cracks occurred at cycle $R=5/1000$, and the beam main bars yielded at cycle $R=10/1000$. From $R=10/1000$ to $20/1000$, all specimens reached the maximum load. In the case of specimens with the same number of beam main bars, the beam and column flexural and joint shear cracking loads and the maximum loads became larger, and the drift angle at beam main bars yielding decreased, with the increasing of F_c . In the specimens with the same F_c , the drift angles and the loads at beam main bars yielding of specimens 2,4 and 6 were larger than those of specimens 1,3 and 5. Specimens 2,4 and 6 had more beam main bars. At $R=20/1000$, the joint shear cracks of specimens 2,4 and 6 were more pronounced. After the maximum load, the joint shear crack width of specimens 2,4 and 6 increased with the increasing drift angle, and finally the cover concrete of the joints segregated by the final cycle. On the other hand the joint shear cracks of specimens 1,3 and 5 did not widen, and the concrete crushed and segregated at the beam compressive regions adjacent to the column face by the final cycle.

In Fig.4, the loss of strength at the second cycle of each drift angle of specimens 1 and 3 became larger than those of specimens 2 and 4 from $R=20/1000$. And this loss of the specimen 5 became larger than that of specimen 6 after $R=30/1000$. The slip in hysteresis loop of specimens 1,3 and 5 was more pronounced than that of specimens 2,4 and 6. The slip of specimens 1,3 and 5 started at $R=20/1000$, $10/1000$, $30/1000$ respectively. Namely with larger F_c , the commencement of slip is later. At all the loadings, the axial load was kept constant until the final cycle.

Reinforcement Strain

The strain distribution of the beam upper main bars through the joint are shown in Fig.5. These values of strain are at the peak of the first forward loading cycle at each drift angle. The beam tensile main bars at

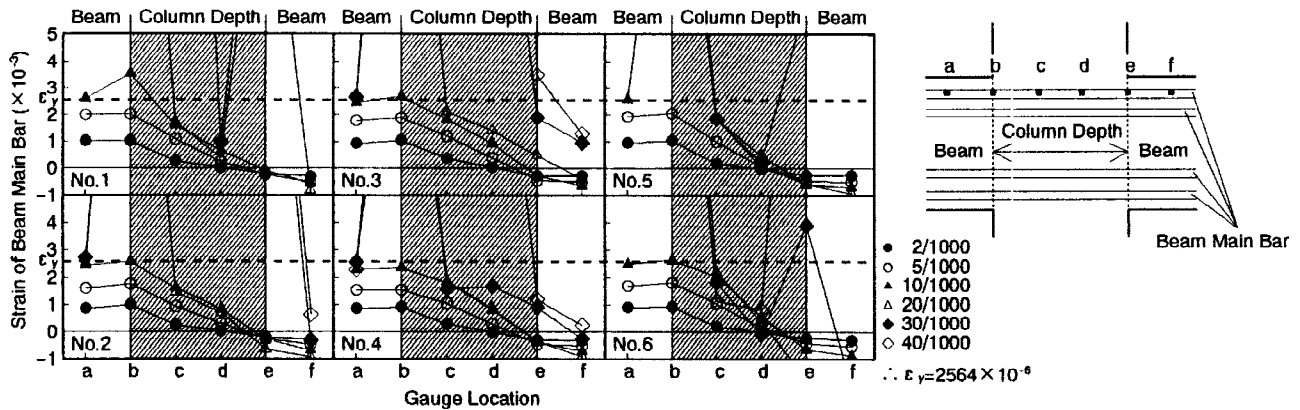


Fig.5. Strain Distributions of Beam Main Bars through a Joint

the critical section (point b) of all the specimens yielded at $R=5/1000$ to $10/1000$. With the exception of specimen 6, as the drift angle increases, the strain at point c reached yield. As for specimens with $F_c=41.2\text{MPa}$, at point c of specimens 3 and 4 yield occurred at $R=20/1000$ to $30/1000$ and $R=30/1000$ to $40/1000$ respectively. Therefore it is believed that bond failure in the joint of specimen 3 occurred earlier than that of specimen 4. In specimen 3, the reason for the loss of strength at the second cycle of $R=20/1000$ may be attributable to bond failure. As for specimens with $F_c=58.5\text{MPa}$, at point c of specimen 5 yield occurred at $R=30/1000$ to $40/1000$. In the case of specimen 5, the reason for the loss of strength at the second cycle of $R=30/1000$ may also be attributable to bond failure. On the other hand, the strain at point c of specimen 6 reached the maximum without yielding at $R=20/1000$, and this strain decreased. As for the specimens with $F_c=35.3\text{MPa}$, at point c of both specimens 1 and 2 yield occurred at $R=20/1000$ to $30/1000$. The loss of strength of specimen 1 was larger than that of specimen 2 at the second cycle of $R=20/1000$. The concrete of specimen 1 crushed at the beams compressive regions of critical sections. Therefore it is believed that the strength of specimen 1 at the second cycle of $R=20/1000$ became smaller than that at the first cycle with bond failure.

Joint Shear Deformation

The contributions of parts of specimens to the total story drift at the first forward cycles are shown in Fig. 6(a). The beam flexural deflection includes the influence of the beam main bars slipping from the joint. In the specimens with the same F_c , the contributions of the joints of specimens 2,4 and 6 were larger than those of specimens 1,3 and 5. In particular, that of specimens 4 and 6 were very large, and increased with increasing deflection.

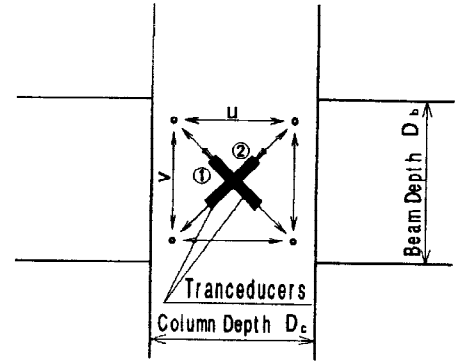
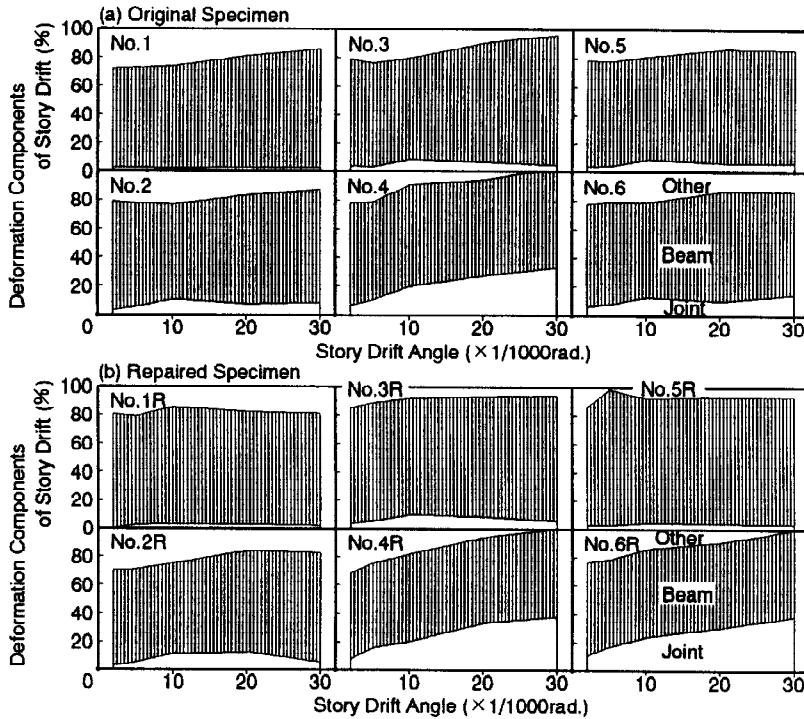
Failure Mode

From the results above, the failure mode of specimens 1,3,5 and 2,4,6 were regarded as "bond splitting failure of the joint after the beam flexural yielding (called BBo)" and "shear compression failure of the joint after the beam flexural yielding (called BJ)" respectively.

COMPARISON BETWEEN SPECIMENS BEFORE AND AFTER REPAIR

Failure Progress During Loading after Repair

Fig.7 shows the crack patterns of repaired specimens at $R=20/1000$. At the places restored with non-shrinking high-strength mortar, the patterns of beam and column flexural cracks and joint shear



$$\theta_j = \frac{1 - D_c}{H(L - D_b)} \cdot \frac{(\delta_1 - \delta_2)\sqrt{u^2 + v^2}}{2uv}$$

- θ_j : joint shear distortion angle
- D_c : column depth (=400mm)
- D_b : beam depth (=400mm)
- L : distance between beam loading points (=2700mm)
- H : distance between points of contraflexure of column (=1500mm)
- u, v : horizontal and vertical measuring distances (=274mm)
- δ_1, δ_2 : deformation of joint at diagonal

Fig.6. Deformation Components of Story Drift

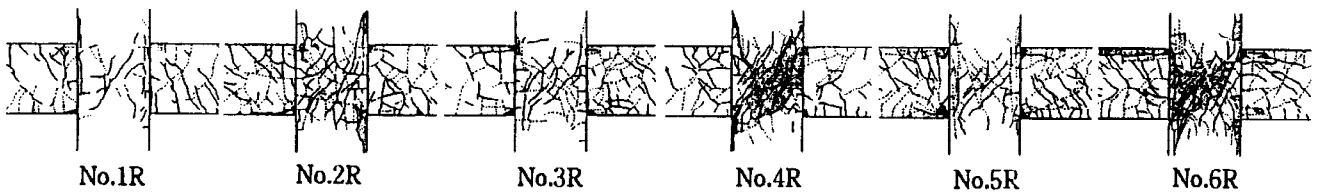


Fig.7. Crack patterns of Repaired Specimens (20/1000rad.)

crack swere similar to the original specimens. At the places without mortar, some cracks due to the original loading opened again. Many shear cracks appeared on the joints of specimens 2R,4R and 6R, and then the cover concrete of the joint segregated by the final cycle in a similar way to the original specimen. The concrete of specimens 1R,3R and 5R crushed and segregated at the critical section of the beams. Therefore it is believed that the bond failure in the joints of these specimens occurred in a similar way to original specimens 1,3 and 5. Throughout the loading after repair, a constant axial load was maintained until the final cycle.

Load-Deflection Curve

The solid lines in Fig.4 show the load-deflection curves during loading after repair. The stiffness of the repaired specimens was one-third that of the original specimens. However, at the first cycle of R=20/1000, the strength of repaired specimens 1R,2R,3R and 5R nearly reached the maximum load of each original specimen. From R=20/1000 the loss of strength with increment of drift angle was small, and the loss of strength at the second cycle of each drift angle of these repaired specimens was smaller than that of the original specimens. At the final cycle, the strength of all the repaired specimens was the same as the original specimens.

Table 5. Stiffness and Maximum Load

Specimen	Secant Stiffness (kN/mm)	Repaired Original	Maximum Load Pmax(kN)	Repaired Original	Drift Angle at Pmax ($\times 1/1000$ rad.)	Repaired Original	Final Failure Mode
No. 1 No. 1R	59.1 21.0	0.35	179.5 163.8	0.91	20.1 16.5	0.82	BBo BBo
No. 2 No. 2R	66.5 21.3	0.32	252.0 214.8	0.85	15.9 20.5	1.29	BJ BJ
No. 3 No. 3R	56.8 15.2	0.27	168.7 161.8	0.96	9.7 20.4	2.10	BBo BBo
No. 4 No. 4R	65.4 16.3	0.25	229.5 183.4	0.80	20.2 70.3	3.48	BJ J'
No. 5 No. 5R	77.3 25.5	0.33	258.9 210.8	0.81	18.9 32.7	1.73	BBo BBo
No. 6 No. 6R	64.1 20.9	0.33	329.5 240.3	0.73	18.7 70.2	3.75	BJ J'

The strain of reinforcement after the original loading was defined as zero. It was concluded that the beam main bars of specimens 1R,2R,3R,5R, and 4R,6R yielded at $R=20/1000$ and $R=40/1000$ respectively. The slip in hysteresis loops of the repaired specimens 1R,3R and 5R were very similar to the originals. From these results, the failure mode of specimens 1R,3R and 5R were regarded as BBo-type.

Stiffness and Maximum Load

The stiffness and maximum loads are listed in Table 5. The stiffness is secant stiffness between the starting point and the measured point just before 27.4kN, which was the smallest of the beam flexural cracking loads during the original loading. The ratios of the stiffness of repaired specimens 3R and 4R to those of original specimens 3 and 4 were 0.27, 0.25. Those of other specimens were 0.32 to 0.35.

The ratios of maximum loads of the repaired specimens to those of the original specimens were 0.73 to 0.96. Except for specimens 4R and 6R whose strength was small at $R=20/1000$, these ratios were 0.81 to 0.96. The ratios of specimens 1R,3R and 5R (original were BBo-type) were larger than those for specimens 2R,4R and 6R (original were BJ-type). The ratios of specimens 1R ($F_c=41.2$ MPa), 3R ($F_c=35.3$ MPa), and 5R ($F_c=58.8$ MPa) were 0.91, 0.96, 0.81 respectively. Namely these ratios became larger with F_c decreased. The reason may be that the ratios of the compressive strength of the mortar (69.6MPa) to σ_B of the original specimens increased as the concrete strength decreased, and this affected the bond strength of the beam main bars.

Joint Shear Deformation

The contribution of parts of the repaired specimens to the total story drift is shown in Fig.6(b). The contributions of the joint of specimens 2R,4R and 6R were larger than those of specimens 1R,3R and 5R respectively. Those of repaired specimens 2R,4R and 6R (originals were BJ-type) were larger than those of each original specimen. In particular the difference between 6R and 6 was considerable.

As mentioned above, it was concluded that the beam main bars of specimen 2R yielded at $R=20/1000$. The contribution of joint shear deformation and the failure progress were nearly equal to those of specimen 2. Therefore the failure mode of 2R was regarded as BJ-type. As for specimens 4R and 6R, it is believed that those were different from BJ-type, and were similar to joint shear failure (called J'), because the strength did not recover at $R=20/1000$, and the beam main bars yielded at $R=40/1000$. The reason for the low recovery of strength of these specimens, may be that the joint distortion of the original specimens 4 and 6 was larger than those of the others, and the concrete of the joint failed hard. Moreover for the specimen 6R, the ratio of the compressive strength of mortar to σ_B was small.

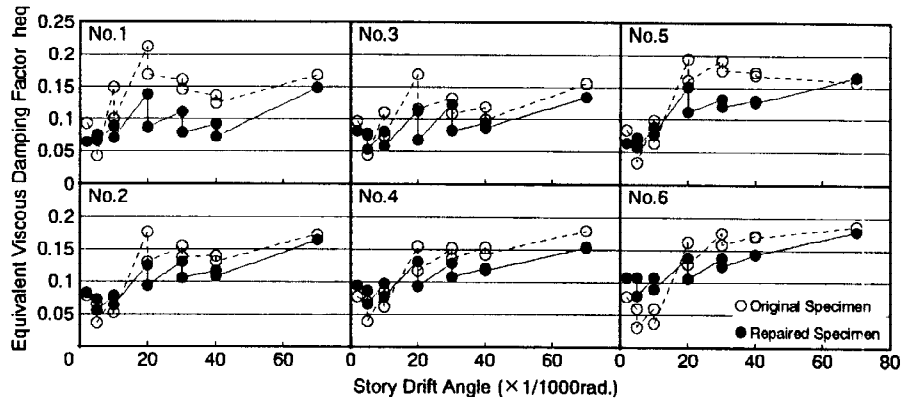


Fig.8. Equivalent Viscous Damping Factor

Equivalent Viscous Damping Factor

The relation between equivalent viscous damping factor heq and story drift angle is shown in Fig 8. In AIJ Design Guidelines (1990), heq is defined as being above 0.1 at $R=20/1000$, and the upper limit of bond index is recommended, so that bond splitting failure of the joint should not occur. The bond indices of all specimens approximate the limit. However, heq of all the original specimens remained over 0.1 not only at the first but also the second cycle of $R=20/1000$. In the specimens with the same number of beam main bars, heq increased, as F_c increased. From $R=20/1000$, heq of the repaired specimens was smaller than heq of the originals. The difference of heq of the BBo-type specimens before and after repair was larger than those of the other types. At the second cycle of $R=20/1000$, though heq of repaired specimens 5R and 6R were over 0.1, the heq of the other specimens were a little less than 0.1.

CONCLUSIONS

The high-strength reinforced concrete interior beam-column joints were repaired using low viscous epoxy resin and non-shrinking high-strength mortar. After repair, a second series of loading tests were carried out. The results are as follows:

- (1) The failure mode of repaired specimens which failed by bond splitting of the joints after flexural yielding of beams (BBo-type) during the original loading, was BBo-type. The failure mode of the repaired specimens which failed by shear compression of the joints after flexural yielding of beams (BJ-type) during the original loading, were BJ-type or similar to shear failure of the joint (J'-type).
- (2) The stiffness of the repaired specimens was one-third that of the original specimens. That maximum load of the repaired specimens whose joint shear deformation was small during the original loading, was 80 to 90% that of the originals.
- (3) The axial load which was applied to the repaired specimens was kept constant until the final cycle. From the maximum load, the loss of strength of the BBo and BJ-type repaired specimens was smaller than the originals.
- (4) The equivalent viscous damping factor of the repaired specimens was about 0.1 at a drift angle of 20/1000 rad.

REFERENCES

- Tasai, A. (1992). Effective repair with resin for bond failure of RC members, The Proceeding 10th WCEE, 5211-5216
- Architectural Institute of Japan (1990). Design Guidelines for Earthquake Resistant Reinforced Concrete Buildings Based on Ultimate Strength Concept, (in Japanese)